

Characterization of woodwind instrument toneholes with the finite element method

Antoine Lefebvre^{a)} and Gary P. Scavone

Computational Acoustic Modeling Laboratory (CAML), Centre for Interdisciplinary Research in Music Media and Technology (CIRMMT), Schulich School of Music, McGill University, 555 Sherbrooke Street West, Montreal, Québec H3A 1E3, Canada

(Received 26 July 2011; revised 16 January 2012; accepted 23 January 2012)

A method is proposed to determine the transfer matrix parameters of a discontinuity in a waveguide with the finite element method (FEM). This is used to characterize open and closed woodwind instrument toneholes and develop expressions for the shunt and series equivalent lengths. Two types of toneholes are characterized: Unflanged toneholes made of thin material, such as found on saxophones and concert flutes, and toneholes drilled through a thick material, such as found on most instruments made of wood. The results are compared with previous tonehole models from the literature. In general, the proposed expressions provide a better fit across a wide range of frequencies and tonehole sizes than previous results. For tall toneholes, the results are in general agreement with previous models. For shorter tonehole heights, some discrepancies from previous results are found that are most important for larger diameter toneholes. Finally, the impact of a main bore taper (conicity) on the characterization of toneholes was investigated and found to be negligible for taper angles common in musical instruments.

© 2012 Acoustical Society of America. [DOI: 10.1121/1.3685481]

PACS number(s): 43.75.Pq [JW]

Pages: 3153–3163

I. INTRODUCTION

The goals of the research presented in this paper are to derive the transfer matrix parameters of woodwind instrument toneholes using the finite element method (FEM), to develop simple formulas valid for any tonehole height and diameter, and to address the potential impact of a main bore taper. The proposed method can also be applied to derive transfer matrix parameters for other discontinuities in a uniform waveguide.

The quality of a woodwind music instrument can be estimated in part by analyzing the frequencies, magnitudes, and harmonicity of its resonances, as well as its tonehole lattice cutoff frequency. This information can be deduced from the input impedance or reflectance of an instrument. The transfer matrix method (TMM) provides an efficient means for calculating the input impedance of a hypothetical air column (Caussé *et al.*, 1984; Keefe, 1990). With the TMM, a geometrical structure is approximated by a sequence of one-dimensional segments, such as cylinders, cones, and closed or open toneholes, and each segment is represented by a transfer matrix (TM) that relates its input to output frequency-domain quantities of pressure (P) and volume velocity (U). The multiplication of these matrices yields a single matrix, which must then be multiplied by an appropriate radiation impedance at its output. That is,

$$\begin{bmatrix} P_{\text{in}} \\ U_{\text{in}} \end{bmatrix} = \left(\prod_{i=1}^n \mathbf{T}_i \right) \begin{bmatrix} Z_{\text{rad}} \\ 1 \end{bmatrix}, \quad (1)$$

where Z_{rad} is the radiation impedance. The input impedance is then calculated as $Z_{\text{in}} = P_{\text{in}}/U_{\text{in}}$.

Among all possible sources of error in the calculation of the input impedance of woodwind instruments using the TMM, the transfer-matrix representation of toneholes is of primary importance. Woodwind instrument toneholes have been theoretically characterized using modal decomposition (Keefe, 1982b; Dubos *et al.*, 1999) and simulated with the finite difference method (FDM) (Nederveen *et al.*, 1998). However, the theoretical characterizations are sometimes limited because the geometries of the toneholes found on real instruments differ to some degree from the idealized geometries for which the models are developed. Indeed, woodwind instrument toneholes may be undercut, rounded off at each end, be noncylindrical, and/or have a keypad suspended above them. Many of these more realistic geometries are too complex to be characterized analytically. For example, previous tonehole models have approximated the saddle-shaped surface at the junction between the air column and the tonehole as planar. This may lead to a small error of unknown magnitude that is increasingly important for larger diameter toneholes. Further, these calculations have not accounted for the coupling between the internal and external discontinuity that occurs when the tonehole height is smaller than its radius. A generic numerical method to estimate the tonehole parameters for any geometry would be useful to determine if any of these features change the parameters of the toneholes in a significant manner and to develop appropriate formulas if this is the case.

In this paper, a method based on the solution of the Helmholtz equation in three dimensions ($\nabla^2 P + k^2 P = 0$) using the FEM is presented. Numerical simulations with the FEM do not suffer from the previously mentioned

^{a)}Author to whom correspondence should be addressed. Electronic mail: antoine.lefebvre2@mail.mcgill.ca

limitations and allow the verification and extension of previous theory. The method involves the solutions of an arbitrary tonehole geometry with two different boundary conditions. The transfer matrix parameters of the discontinuity are then obtained from these solutions by solving a system of linear equations. This approach may be applied to arbitrary geometries, enabling the characterization of various discontinuities, such as toneholes, constrictions, and diameter mismatches.

Two types of toneholes commonly found in woodwind instruments are characterized in this paper: (1) An unflanged tonehole made of thin material, such as found on saxophones and concert flutes and (2) a tonehole drilled through a thick material, such as found on the clarinet, oboe, recorder, and most instruments made of wood (see Fig. 1). Based on the FEM results, formulas are proposed and compared to previous results from the literature. Here, the objective is to propose the most simple formulas that are accurate enough for the problem of designing woodwind instruments, rather than formulas that “exactly” fit the FEM results.

The calculation of the input impedance of woodwind instruments using the TMM ignores internal and external tonehole interactions. It is assumed that the toneholes are located sufficiently far from each other that the evanescent modes excited near one tonehole do not interact with those of adjacent toneholes, a condition that becomes more problematic on instruments with larger toneholes that are spaced more closely together. It is also assumed that the sound radiated from one tonehole does not interact with the radiated sound from other open toneholes, as if they are radiating in different spaces. Therefore, input impedances calculated using the TMM and the formulas presented in this paper are expected to differ to some degree from measurements on woodwind instruments. Nevertheless, the characterization of the single woodwind instrument tonehole remains fundamental and the basis for further improvements.

II. TONEHOLE TRANSMISSION MATRIX

The tonehole TM can be approximated as a symmetric T section (see Fig. 2) depending on two parameters, the shunt impedance Z_s and the series impedance Z_a . The TM of the tonehole is written as (Keefe, 1982b)

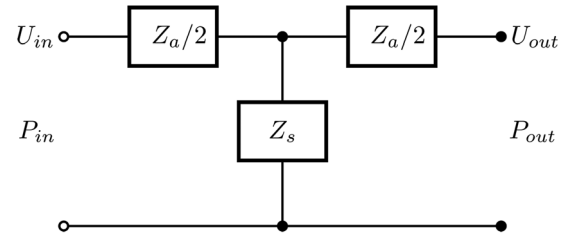


FIG. 2. Transmission matrix representation of a symmetric tonehole.

$$\mathbf{T}_{\text{hole}} = \begin{bmatrix} 1 + \frac{Z_a}{2Z_s} & Z_a \left(1 + \frac{Z_a}{4Z_s} \right) \\ 1/Z_s & 1 + \frac{Z_a}{2Z_s} \end{bmatrix}. \quad (2)$$

The shunt and series impedances may be expressed in terms of equivalent lengths t_s and t_a . For an open tonehole state [superscript (o)],

$$Z_s^{(o)} = Z_{0h} (jkt_s^{(o)} + \xi), \quad (3)$$

$$Z_a^{(o)} = jkZ_0 t_a^{(o)} \quad (4)$$

and for a closed state [superscript (c)],

$$Y_s^{(c)} = jkt_s^{(c)} / Z_{0h}, \quad (5)$$

$$Z_a^{(c)} = jkZ_0 t_a^{(c)}, \quad (6)$$

where $Z_0 = \rho c / \pi a^2$ is the characteristic impedance of an assumed cylindrical primary air column of radius a , $Z_{0h} = \rho c / \pi b^2$ is the characteristic impedance of the tonehole of radius b , $k = 2\pi f / c$ is the wavenumber, f is the frequency, ρ and c are, respectively, the density of air and the velocity of sound in air, and ξ characterizes radiation losses when the tonehole is open. For an unflanged pipe, $\xi = (kb)^2 / 4$ is a low frequency approximation (Dalmont *et al.*, 2002).

To evaluate $Z_s^{(o)}$, Dalmont *et al.* (2002) proposed the following:

$$Z_s^{(o)} = jZ_{0h} \{ kt_i + \tan[k(t + t_m + t_r)] \}, \quad (7)$$

where t is the physical height, t_i is the inner length correction, t_m is the matching volume length correction, and t_r the

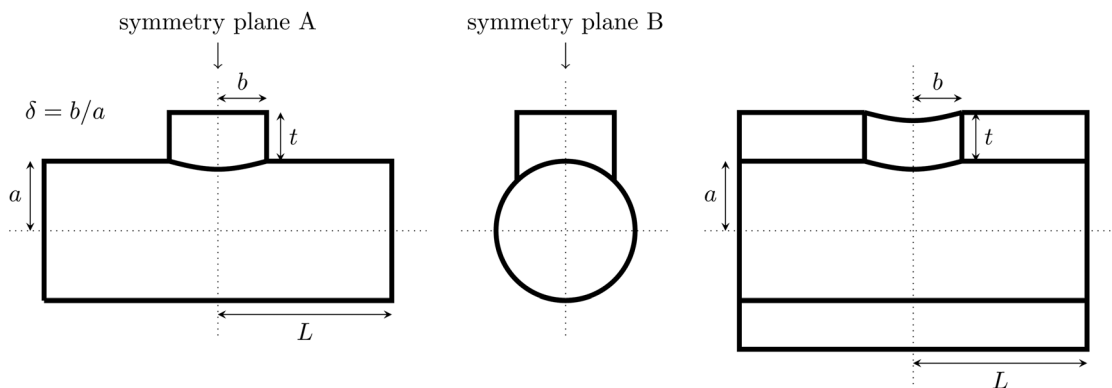


FIG. 1. Diagram representing a tonehole on a pipe: Unflanged tonehole on the left, tonehole on a thick pipe on the right.

radiation length correction. The matching volume length correction is calculated with (Nederveen *et al.*, 1998)

$$t_m = b\delta(1 + 0.207\delta^3)/8. \quad (8)$$

The radiation length correction is obtained from the radiation impedance Z_r of the opening with (Dalmont *et al.*, 2002)

$$t_r = \arctan[Z_r/(jZ_{0h})]/k. \quad (9)$$

This is a complex quantity that includes the effect of radiation losses. For an unflanged tonehole, the model of an unflanged pipe in the low frequency approximation is satisfactory,

$$Z_r = Z_{0h}[0.25(kb)^2 + jk0.61b]. \quad (10)$$

For a tonehole drilled through a thick pipe, a formula for the radiation length correction was proposed by Dalmont and Nederveen (2001),

$$\delta_{cyl} = 0.822 - 0.47[b/(a+t)]^{0.8}. \quad (11)$$

This result was experimentally validated by Dickens (2007).

A data-fit formula for the inner length correction t_i based on simulation results using the FDM was proposed by Nederveen *et al.* [1998, Eq. (40)],

$$t_i = (0.82 - 1.4\delta^2 + 0.75\delta^{2.7})b. \quad (12)$$

A theoretical equation based on modal decomposition was also reported by Dubos *et al.* [1999, Eq. (73)],

$$t_i = (0.82 - 0.193\delta - 1.09\delta^2 + 1.27\delta^3 - 0.71\delta^4)b - t_a^{(o)}/4, \quad (13)$$

where the series equivalent length $t_a^{(o)}$ is defined in the upcoming Eq. (15).

For the series equivalent length $t_a^{(o)}$ of an open tonehole, Nederveen *et al.* (1998, Fig. 11) proposed a formula based on the results of simulations with the FDM,

$$t_a^{(o)} = -0.28b\delta^2. \quad (14)$$

Using modal decomposition, Dubos *et al.* [1999, Eq. (74)] gave

$$t_a^{(o)} = -\frac{b\delta^2}{1.78 \tanh(1.84t/b) + 0.940 + 0.540\delta + 0.285\delta^2}. \quad (15)$$

For closed toneholes, the shunt impedance is given by Nederveen (1998),

$$Z_s^{(c)} = jZ_{0h}[kt_i - \cot[k(t+t_m)]], \quad (16)$$

where the inner length correction t_i is negligible at low frequencies and is often ignored.

For the series equivalent length $t_a^{(c)}$ of a closed tonehole, Nederveen [1998, Eq. (A3.5)] proposed

$$t_a^{(c)} = -(2t/\pi b) \arctan(b/2t)b\delta^2, \quad (17)$$

whereas Dubos *et al.* [1999, Eq. (74)] gave

$$t_a^{(c)} = -\frac{b\delta^2}{1.78 \coth(1.84t/b) + 0.940 + 0.540\delta + 0.285\delta^2}. \quad (18)$$

The series equivalent length of a closed tonehole is equal to that of an open tonehole when $t > b$. For instance, Eqs. (15) and (18) give the same results when $t/b \rightarrow \infty$ (Dubos *et al.*, 1999),

$$t_a^{(o,c)} = -(0.37 - 0.087\delta)b\delta^2. \quad (19)$$

For instruments played directly with the fingers, there exists a negative length correction caused by the reduction of the tonehole volume by the finger, which protrudes inside it. A modification to Eq. (18) was given by Dickens (2007) to account for this effect. In this study, no attempt was made to model the presence of a finger. In general, when the tonehole height t is shorter than its radius b , a dependence of the shunt and series impedances over t is expected.

III. ESTIMATION OF THE REQUIRED ACCURACY OF THE EQUIVALENT LENGTHS

In this section, the acceptable error in the parameters of the transfer matrix of open or closed toneholes is estimated using the theory and notation presented by Nederveen (1998, Sec. 32). Based on pitch discrimination results of Hartmann (1996), a maximum tolerable error in the calculation of the playing frequencies is assumed to be ± 5 cents (0.3%), whereas ± 1 cent (0.06%) is below the threshold of audibility. A tolerance of 0.2% appears reasonable.

The playing frequencies of wind instruments are determined by the coupling between a nonlinear generator and the linear response of the instrument. The physics of this complex problem have been the subject of many publications; see Fletcher (1999) for a summary. For the purpose of this paper, it is assumed that the playing frequency is directly related to the resonance frequencies of the instrument, including a length correction to approximate the effect of the generator. That is, it is assumed that an error of 0.2% in the estimation of the resonance frequencies will lead to an error of 0.2% in the playing frequencies, which is likely not exactly the case but should be relatively close.

For the shunt equivalent length of an open tonehole $t_s^{(o)}$, this error can be evaluated from a first order approximation. It is assumed that the tonehole shifts the frequency by one semitone, so that $L_c/L_o = (1+g) \approx 1.06$, where L_c is the acoustic length of the tube when the tonehole is closed and L_o is the acoustic length when the tonehole is open. The acoustic length L is related to the first resonance frequency with $L = c/2f$ for conical reed instruments and flutes and $L = c/4f$ for cylindrical reed instruments. It is possible to

calculate the derivative of the tonehole equivalent length with respect to a change in the acoustic length of the instrument, that is, how much the tonehole equivalent length should increase to produce a unit change in the acoustic length of the instrument,

$$\frac{dt_s^{(o)}}{dL_o} = \delta^2(1-z)\sqrt{1+4\lambda/gL_o}, \quad (20)$$

where $\lambda = t_s^{(o)}/\delta^2$ and $z = 0.5g(\sqrt{1+4\lambda/gL_o} - 1)$. The maximal error in the open tonehole shunt equivalent length is

$$\Delta t_s^{(o)} = \frac{dt_s^{(o)}}{dL_o} \Delta L_o, \quad (21)$$

with $\Delta L_o = 0.002L_o$ (0.2% accuracy).

The error $\Delta t_s^{(o)}$ was calculated for varying geometries and lengths L_o . The acceptable error varies with geometry. In general, a wider and taller tonehole can tolerate a larger error in its equivalent length. An accuracy of $0.2b$ on the shunt equivalent length is found to be acceptable in most cases.

For the open series equivalent length, the required accuracy is

$$\Delta t_a^{(o)} = \frac{dt_a^{(o)}}{dL_o} \Delta L_o \approx 0.002L_o, \quad (22)$$

because $t_a^{(o)}$ represents a change in acoustic length.

In the case of closed toneholes, all of the toneholes located before the first open tonehole have an influence on the resonance frequency of the instrument. Thus, there is a cumulative effect and the worse case always occurs for the lowest note of an instrument. In the case of the closed shunt impedance, the maximal error is calculated approximately from a simplification of Eqs. (35.12-13) from [Nederveen \(1998\)](#), which yields

$$\Delta t_s^{(c)} = \frac{dt_s^{(c)}}{dL_c} \Delta L_c \approx \frac{4}{N\delta^2} \times 0.002L_c, \quad (23)$$

and for the series length correction term,

$$\Delta t_a^{(c)} = \frac{dt_a^{(c)}}{dL_c} \Delta L_c \approx \frac{1}{N} \times 0.002L_c, \quad (24)$$

where N is the number of toneholes on the instrument.

In Sec. VI, these estimated values are used to display the range of validity of the various length corrections in the figures using gray regions.

IV. FEM PROCEDURE

The FEM allows a three-dimensional representation of a geometric structure with coupled internal and external domains, taking into account any complexities of the geometry under study with no further assumptions. For all the simulations, curved third-order Lagrange elements are used. All open simulated geometries include a surrounding spherical

radiation domain that uses a second-order nonreflecting spherical-wave boundary condition on its surface, as described by [Bayliss et al. \(1982\)](#). Further discussion of this topic can be found in [Tsynkov \(1998\)](#) and [Givoli and Neta \(2003\)](#). The effect of the thermoviscous losses is negligible for most woodwind instrument toneholes because the boundary layer thickness is small relative to their size and because they are short in height. Therefore, no attempt was made to account for such losses in this study. As well, results from the literature do not include the effect of losses and thus, inclusion of such would complicate the comparisons. That said, thermoviscous losses can be included in the FEM simulations if desired ([Kampinga et al., 2010](#)). The simulations were performed with a speed of sound $c = 343$ m/s and a density $\rho = 1.25$ kg/m³.

A commercial FEM software package was validated with the simulation of a flanged and an unflanged pipe radiating into a sphere with the aforementioned boundary condition. The radiation impedance was calculated for values of ka varying from 0.1 to 1 (from 546.9 to 5459 Hz) in steps of 0.1 with an additional low-frequency point at 0.01 (54.6 Hz). The refinement of the mesh along geometry discontinuities is critical to the accuracy of the solution (mainly for the imaginary part). It was found that 100 elements along the circular edge where the pipe ends produce good results. The total number of degrees of freedom for the validation models and the tonehole models varied between 30 000 and 80 000 depending on the geometry. The end corrections were found to be in agreement with theory ([Levine and Schwinger, 1948](#); [Norris and Sheng, 1989](#)) to great accuracy ([Lefebvre, 2010](#)). The error is less than 0.1% for the low frequency point and less than 0.5% for all frequencies for the unflanged case; for the flanged pipe, the results were compared with an approximate formula from [Norris and Sheng \(1989\)](#) and the error is around 2% for the highest frequency point, which may be in part an error in the approximate formula used for the verification. The error on the real part is less than 0.1% for the low frequency point in both cases; it is less than 1% for all frequencies in the unflanged case and less than 3% for the flanged case.

For the purposes of this paper, the results of the FEM simulations must be transformed to a TM characterization of the object under study (T_{obj}). The TM method is useful to characterize any type of discontinuity embedded in a waveguide, i.e., which has an input and an output plane. One requirement is that the evanescent modes occurring near the discontinuity must be sufficiently damped at the input and output planes of the simulated model. Thus, cylindrical segments are required in the FEM simulations before and after the discontinuity. The lengths of these segments is specified as five times the input radius in order to ensure the evanescent modes have decayed by a factor of more than 1×10^{-3} , based on the theory of guided waves ([Pierce, 1989](#)). That being said, as mentioned in the introduction, the distance between adjacent toneholes on woodwind instruments is often insufficient for this condition to be fully met; this means that the evanescent modes excited near a tonehole interact with the other toneholes, an effect that limits the accuracy of calculations based on the transfer matrix method.

The transfer matrix \mathbf{T} obtained from the simulations is that of the complete cylinder–object–cylinder system. It contains four frequency-dependent, complex-valued parameters relating input quantities to output quantities of pressure (P) and volume velocity (U). In order to obtain these four parameters from the FEM results, the problem has to be simulated two times with different boundary conditions. By combining the results for the two simulation cases (subscripts 1 and 2), a system of linear equations is written to solve for the four parameters of the transfer matrix,

$$\begin{bmatrix} P_{\text{out}1} & U_{\text{out}1} & 0 & 0 \\ 0 & 0 & P_{\text{out}1} & U_{\text{out}1} \\ P_{\text{out}2} & U_{\text{out}2} & 0 & 0 \\ 0 & 0 & P_{\text{out}2} & U_{\text{out}2} \end{bmatrix} \begin{bmatrix} T_{11} \\ T_{12} \\ T_{21} \\ T_{22} \end{bmatrix} = \begin{bmatrix} P_{\text{in}1} \\ U_{\text{in}1} \\ P_{\text{in}2} \\ U_{\text{in}2} \end{bmatrix}. \quad (25)$$

The transfer matrix made of these coefficients can be expressed as $\mathbf{T} = \mathbf{T}_{\text{cyl}1} \mathbf{T}_{\text{obj}} \mathbf{T}_{\text{cyl}2}$, where the TM of a cylindrical duct is

$$\mathbf{T}_{\text{cyl}} = \begin{bmatrix} \cos kL & jZ_0 \sin kL \\ j \sin kL / Z_0 & \cos kL \end{bmatrix}. \quad (26)$$

The effect of the cylinders is removed by calculation using the inverse of the cylinder’s transfer matrix to obtain the coefficients of the matrix \mathbf{T}_{obj} of the object under study. Finally, making use of Eq. (2), the shunt and series impedances are retrieved.

If the object under investigation is symmetric, only one-half of the geometry is solved (see Fig. 1). On symmetry plane A, two boundary conditions are defined alternately: A null normal acceleration for the symmetric case (case 1) and a null pressure for the anti-symmetric case (case 2). From the values of the pressure and normal velocity on the input plane of the model, the values on the output plane for both simulation cases are deduced,

$$P_{\text{out}1} = P_{\text{in}1}, \quad (27)$$

$$U_{\text{out}1} = -U_{\text{in}1}, \quad (28)$$

$$P_{\text{out}2} = -P_{\text{in}2}, \quad (29)$$

$$U_{\text{out}2} = U_{\text{in}2}. \quad (30)$$

The model of a tonehole has another symmetry (plane B) so that only one-quarter of the geometry is required. A typical geometry and mesh for an unflanged tonehole is shown in Fig. 3.

Dalmont *et al.* (2002) used a similar method, but simplified the problem by assuming the symmetry condition $T_{11} = T_{22}$ and the reciprocity condition $T_{11}T_{22} - T_{12}T_{21} = 1$. That simplification is not used in this study because it does not work for a tonehole on a conical bore and because it is not necessary in a numerical approach, where both pressures and velocities are available. For a symmetric system, the calculation method that is proposed requires two solutions of a model that is one-half the size, which takes less time and memory than the solution of a single larger model. The

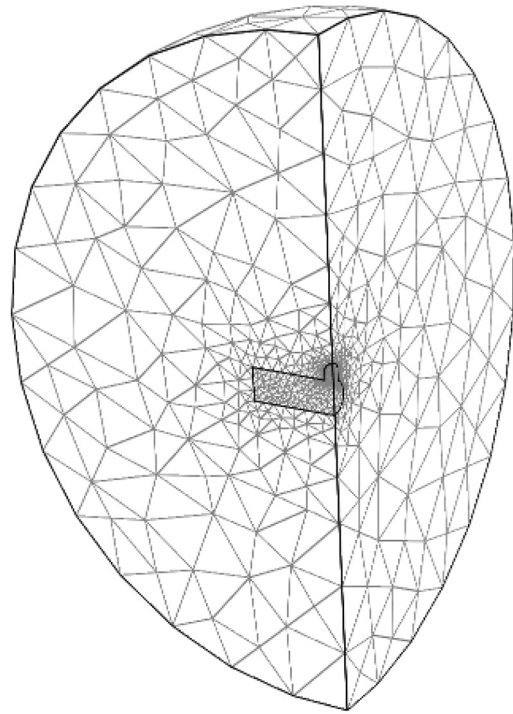


FIG. 3. Typical mesh for the case of a tonehole on a cylindrical pipe.

approach used by Keefe (1982a) is based on the displacement of the resonance frequencies and gives results only at discrete frequency points.

V. FEM TONEHOLE MODEL VALIDATION

The FEM simulation results are compared with the experimental data obtained by Dalmont *et al.* (2002) and Keefe (1982a). Dalmont *et al.* (2002) measured the shunt and series equivalent lengths of a single tonehole on a pipe of radius $a = 10$ mm as a function of frequency for two different tonehole geometries: (1) $\delta = 0.7$, $t/b = 1.3$ and (2) $\delta = 1.0$, $t/b = 1.01$. They also measured the real part of the shunt impedance for the larger diameter tonehole. Both tonehole geometries were flanged at their open end. The FEM results are also compared with data obtained by Keefe (1982a), who measured the shunt and series equivalent lengths of a single unflanged tonehole on a cylinder of radius $a = 20$ mm for two tonehole geometries: (1) $\delta = 0.66$, $t/b = 0.48$ and (2) $\delta = 0.32$, $t/b = 3.15$.

The shunt equivalent length $t_s^{(o)}$ as a function of ka (in steps of 0.05) obtained from the FEM simulations is displayed in Figs. 4 and 6 in comparison to these experimental results. The FEM results are in good general agreement with the experimental results of Dalmont *et al.* (2002). In the lower frequency range, the FEM results match the theoretical results. In the results of Dalmont *et al.* (2002), the equivalent length is found to be 0.6 ± 0.3 mm larger than predicted for $\delta = 1$ and 0.5 ± 0.3 mm for $\delta = 0.7$. The FEM results do not show this trend. In the higher frequency range, it is found that the equivalent length becomes larger than predicted with previous results, indicating a frequency dependence of the inner length correction, in accordance with the experimental results of Dalmont *et al.* (2002).

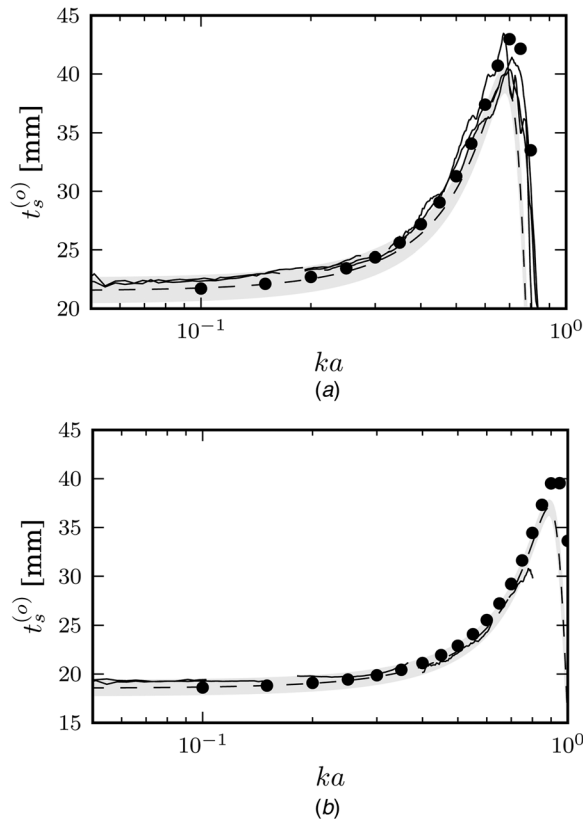


FIG. 4. Shunt length correction $t_s^{(o)}$ as a function of ka for the two toneholes studied by [Dalmont et al. \(2002\)](#): $\delta = 0.7$ and $t/b = 1.3$ (top graph), $\delta = 1.0$, $t/b = 1.01$ (bottom graph). FEM results (filled circles), experimental data from [Dalmont et al. \(2002\)](#) (solid line) and theoretical results with Eqs. (3) and (7) (dashed line).

The real part of the shunt impedance obtained from the FEM simulations is displayed in Fig. 5 in comparison to the experimental results of [Dalmont et al. \(2002\)](#) and theoretical calculations without viscothermal losses. The FEM and experimental results are in general agreement. The real part appears to be slightly larger than predicted by theory near the maximum.

In the case of the unflanged toneholes studied by [Keefe \(1982a\)](#), good agreement is found between the theoretical values, the FEM results and his experimental data for the

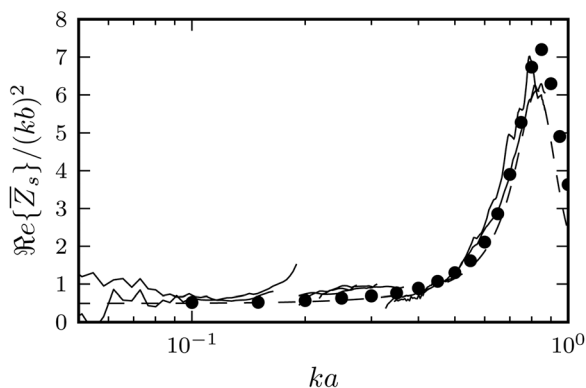


FIG. 5. Real part of the shunt impedance divided by $(kb)^2$ as a function of ka for the tonehole of $\delta = 1.0$ studied by [Dalmont et al. \(2002\)](#). FEM results (filled circles), experimental data from [Dalmont et al. \(2002\)](#) (solid line) and theoretical results with Eq. (7) (dashed line).

tonehole of tall height (see Fig. 6). For the unflanged tonehole of short height, there are discrepancies: The experimental data and the FEM results give larger shunt equivalent lengths for the higher frequencies compared to the theory, even though the experimental data does not quite fit the FEM results. As noted by [Dalmont et al. \(2002\)](#), Eq. (7) is valid when $t > b$. The tonehole of short height in Fig. 6 is shorter than its radius; the discrepancies confirm that the model is not valid in this case and suggest that the inner length correction is frequency dependent.

For the large-diameter tonehole ($\delta = 1.0$), [Dalmont et al. \(2002\)](#) found a series equivalent length $t_a^{(o)}$ of 2.8 ± 0.3 mm, whereas the FEM result is 2.90 mm. For the smaller tonehole ($\delta = 0.7$), their results ($t_a^{(o)} = 0.95 \pm 0.3$ mm) and the FEM result (1.02 mm) are in agreement.

[Keefe \(1982a\)](#) found a value of $t_a^{(o)} = 0.8 \pm 0.2$ mm for the large-diameter ($\delta = 0.66$) tonehole. The FEM result is 0.78 mm. For the small-diameter ($\delta = 0.32$) tonehole, [Keefe \(1982a\)](#) found that no series length correction was experimentally detectable. The FEM result is 1.9×10^{-5} mm, which also confirms this result.

When the large-diameter tonehole is closed by a brass plate, [Keefe \(1982a\)](#) found a shunt equivalent length of $t_a^{(c)} = 6.2 \pm 0.4$ mm, whereas the value from the FEM is 7.55 mm. The theoretical value $t + t_m$ is 7.49 mm. When the tonehole was closed with a standard wind instrument leather pad, [Keefe \(1982a\)](#) reported a smaller value of $t_a^{(c)} = 5.4 \pm 0.2$ mm. This is a rather significant difference (maximal tolerable error approximately 1 mm), which deserves further experimental verification. Similarly, the FEM gives a closed tonehole series equivalent length of $t_a^{(c)} = 0.64$ mm, whereas [Keefe \(1982a\)](#) measured a value of 0.3 ± 0.2 mm when closed by a brass plate and 0.4 ± 0.2 mm when closed by a standard wind instrument leather pad. The accuracy that is required, based on the analysis in Sec. III, is ~ 0.1 mm. Closed toneholes have received little attention compared to open toneholes and the experimental results of [Keefe \(1982a\)](#) do not fit with the FEM or theoretical results. Therefore, further experimental examination appears necessary.

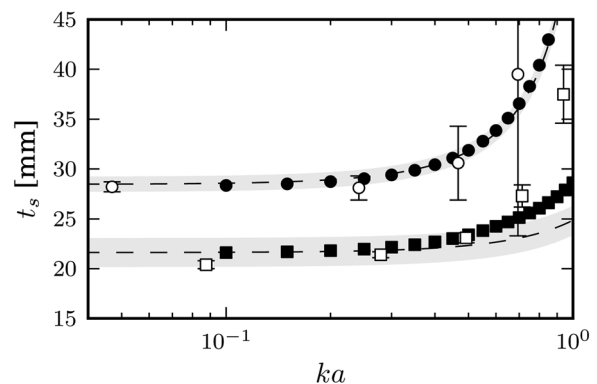


FIG. 6. Shunt equivalent length $t_s^{(o)}$ as a function of ka for the two toneholes studied by [Keefe \(1982a\)](#): $\delta = 0.66$ and $t/b = 0.48$ (bottom curves), $\delta = 0.32$ and $t/b = 3.15$ (top curves). FEM results: For $\delta = 0.66$ (filled circles) and for $\delta = 0.32$ (filled squares). Experimental data from [Keefe \(1982a\)](#) (markers with error bar) and theoretical results with Eqs. (3) and (7) (dashed line).

VI. RESULTS

In this section, the results of FEM simulations for the characterization of both types of toneholes, as depicted in Fig. 1, are presented.

The toneholes were simulated using the FEM for a wide range of geometric parameters ($\delta = b/a$ from 0.1 to 1.0 in steps of 0.05, t/b from 0.1 to 0.3 in steps of 0.05 and from 0.3 to 1.3 in steps of 0.2 and ka from 0.1 to 1.0 in steps of 0.05 with an additional low-frequency point at $ka=0.01$). The lowest frequency simulated was 55 Hz. For all parameters, the four terms of the transfer matrix were obtained and the shunt and series length corrections calculated using the procedure previously described in Sec. IV. Accurate data-fit formulas were previously reported (Lefebvre, 2010), although they exceed the accuracy requirements for the design of music instruments, as defined in Sec. III. In this paper, revised equations that are as simple as possible within the specified error tolerance are presented.

From the simulation results, an expression for the inner length correction was deduced (Lefebvre, 2010),

$$t_i/b = 0.822 - 0.095\delta - 1.566\delta^2 + 2.138\delta^3 - 1.640\delta^4 + 0.502\delta^5. \quad (31)$$

Figure 7 compares this equation with those of the literature; they are very similar to each other.

A. Open toneholes

In Fig. 8, the simulation results for the low-frequency value of the total open shunt length correction $(t_i + t_m + t_r)/b$ is shown for the two extreme cases of short and tall toneholes of both types. For the unflanged toneholes, the effect of the tonehole height is only apparent for holes of small diameter. This can be attributed to variations in the radiation length correction with varying height but the effect is negligible, as indicated by the gray area of validity. For a tonehole drilled through a thick pipe, the radiation length correction is calculated with Eq. (11). The simulation results are in good agreement with the formula found in the literature, confirming their validity.

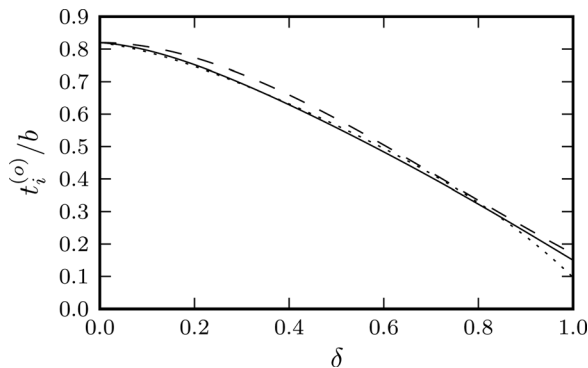


FIG. 7. Comparison of the inner length corrections t_i : Equation (12) (dashed line), Eq. (13) (dotted line), and Eq. (31) (solid line).

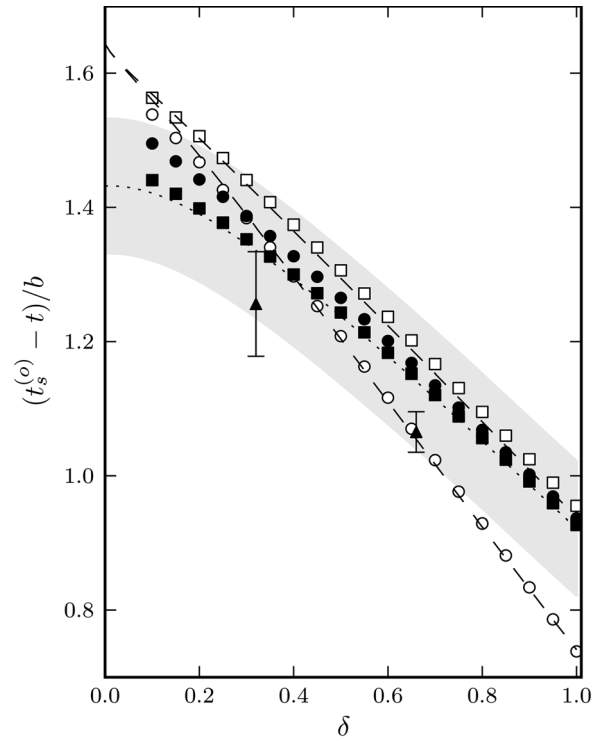


FIG. 8. Total open shunt length correction $(t_s^{(o)} - t)/b = (t_i + t_m + t_r)/b$ as a function of δ . FEM results: Unflanged tonehole (filled markers) and tonehole on a thick pipe (unfilled markers); tall $t=2b$ (squares), and short $t=0.1b$ (circles) toneholes. Experimental data from Keefe (filled triangles with error bars). Model for an unflanged tonehole: Sum of Eqs. (31) and $t_r/b=0.61$ (dotted line), with its validity range in gray. Model for a tonehole on a thick pipe: Sum of Eqs. (31), (8), and (11) (both dashed lines).

From the simulation results, it appears that the inner length correction is frequency dependent. A multiplicative factor $G(\delta, ka)$, which is a function of δ and ka , can be multiplied by the expression for t_i to capture this frequency dependence,

$$G(\delta, ka) = [1 + H(\delta)I(ka)], \quad (32)$$

where

$$H(\delta) = 1 - 4.56\delta + 6.55\delta^2$$

and

$$I(ka) = 0.17ka + 0.92(ka)^2 + 0.16(ka)^3 - 0.29(ka)^4.$$

The open shunt impedance for any tonehole height and diameter can be calculated with Eq. (7) using the inner length correction of Eq. (31) multiplied by the factor of Eq. (32). Figures 9 and 10 show $t_s^{(o)}$ for two different tonehole heights, both with and without the factor G . The frequency-dependent inner length correction better matches the FEM results, which is particularly significant for toneholes with a larger diameter (large value of δ).

In the simulation results, the real part of the open shunt impedance was found to be equal to $0.25(kb)^2$ for all toneholes with a maximal deviation of 1.5%.

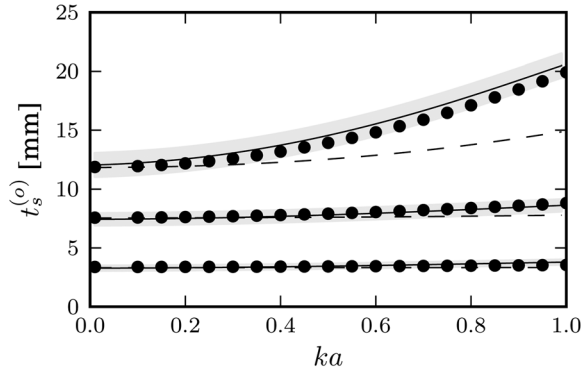


FIG. 9. Shunt equivalent length $t_s^{(o)}$ in millimeters as a function of ka for three values of δ (0.2, 0.5, and 1.0, from bottom to top curve) and a value of $t = 0.25b$ for an unflanged tonehole. FEM results (filled circles). Model: $t_s^{(o)} = Z_s^{(o)} / (jkZ_{0h})$ with $Z_s^{(o)}$ evaluated using Eq. (7) where t_i is evaluated with Eq. (31) (dashed line) and with Eq. (32) (solid line). Validity range in gray.

The low-frequency value of the open tonehole series length correction does not need to be known with great accuracy because of its small impact on the resonance frequencies of woodwind instruments. This is shown in Fig. 11 for both types of toneholes and for the two extreme cases of short and tall chimney heights. The results for both types of toneholes are almost identical. Equation (15) from Dubos *et al.* (1999) is in relative agreement with the simulation results for toneholes of tall height but not for toneholes of short height. The following fit formula matches the simulation results:

$$t_a^{(o)} / b\delta^2 = -0.35 + 0.06 \tanh(2.7t/b). \quad (33)$$

B. Closed toneholes

The FEM results for closed toneholes confirm that the shunt length correction is very well represented by the length $t + t_m$, i.e., by the volume of the tonehole. The effect of the inner length correction grows in importance with frequency.

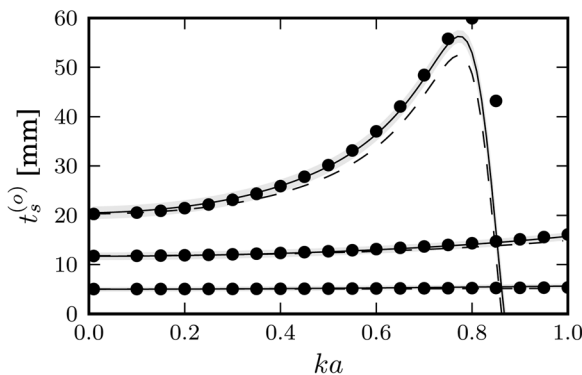


FIG. 10. Shunt equivalent length $t_s^{(o)}$ in millimeter as a function of ka for three values of δ (0.2, 0.5, and 1.0, from bottom to top curve) and a value of $t = 1.1b$ for an unflanged tonehole. FEM results (filled circles). Model: $t_s^{(o)} = Z_s^{(o)} / (jkZ_{0h})$ with $Z_s^{(o)}$ evaluated using Eq. (7) where t_i is evaluated with Eq. (31) (dashed line) and with Eq. (32) (solid line). Validity range in gray.

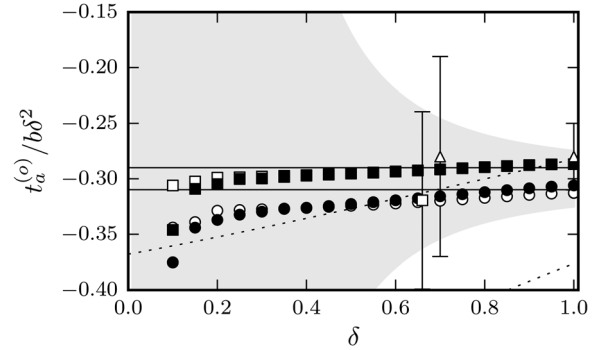


FIG. 11. Series length correction $t_a^{(o)} / b\delta^2$ as a function of δ . FEM results: Unflanged tonehole (filled markers) and tonehole on a thick pipe (unfilled markers, mostly hidden); tall $t = 2b$ (squares) and short $t = 0.1b$ (circles) toneholes. Data fit formula Eq. (33) (solid line) with validity range in gray, and theoretical Eq. (15) (dotted line) for $t = 2b$ and $t = 0.1b$ (see lower right-hand corner). Data points by Keefe (1982a) (unfilled square with error bar) and by Dalmont *et al.* (2002) (unfilled triangles with error bar).

Figure 12 shows the FEM results in comparison with Eq. (16), with and without the term t_i , confirming that t_i can be ignored at low frequency.

Figure 13 displays the series length correction $t_a^{(c)}$ of closed toneholes of both types for the two extreme cases of short and tall chimney heights [using the data fit formula given by the upcoming Eq. (34)]. Equation (18) from Dubos *et al.* (1999) is in good agreement with the simulation results, as was expected because the theoretical development of Dubos *et al.* (1999) was based on an exact formulation of Green's function. The results for the tall tonehole are the same as for an open hole (see Fig. 11), as expected. When the toneholes are short in height, the series length correction term diminishes in magnitude in a different manner depending on the type of tonehole,

$$t_a^{(c)} / b\delta^2 = -0.12 - 0.17 \tanh(2.4t/b). \quad (34)$$

The dependence of the series length correction of an open or closed tonehole on the tonehole height is most important for toneholes of large diameter (as indicated by the region of validity). This is displayed in Fig. 14 for both types of tonehole

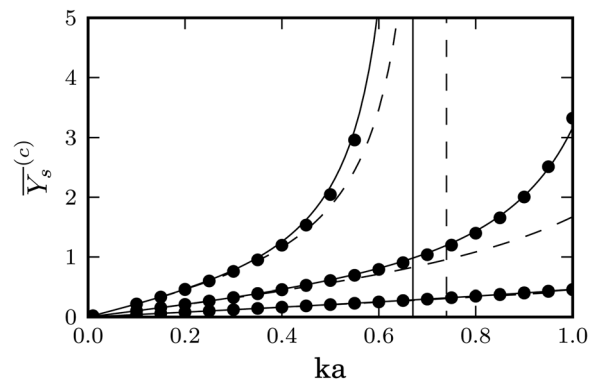


FIG. 12. Shunt admittance of a closed tonehole as a function of ka for three values of δ (0.2, 0.5, and 1.0, from bottom to top curve) and $t = 2b$. FEM results (filled circles). Model: Equation (16) with $t_i = 0$ (dashed line) and with t_i defined by Eq. (31) (solid line).

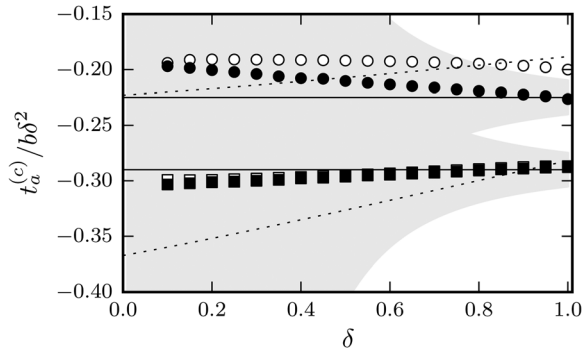


FIG. 13. Series length correction $t_a^{(c)}/b\delta^2$ as a function of δ . FEM results: Unflanged tonehole (filled markers) and tonehole on a thick pipe (unfilled markers, partly hidden); tall $t=2b$ (squares) and short $t=0.1b$ (circles). Data fit formula Eq. (34) (solid line) with validity range in gray. Theory: Equation (18) (dotted line).

with $\delta = 1.0$. For an open tonehole, Eq. (15) overestimates the magnitude of the series equivalent length for toneholes of short height. The use of Eq. (33) is expected to improve results for instruments with toneholes of large diameter and short height. For a closed tonehole, Eq. (18) matches relatively well the simulation results. Equation (17) overestimates the magnitude for tall toneholes. The new data fit formula, Eq. (34), better matches the simulation results of an unflanged tonehole. In all cases of short toneholes, the dependence on t is sufficiently important to cause errors in the evaluation of the resonance frequencies of an instrument with many closed toneholes if it is not accounted for, due to the cumulative effect (Debut *et al.*, 2005). For a saxophone, an error of 25 cents in the estimation of the lowest resonance was found when using Eq. (14) or (19), which are only valid for a closed tonehole when $t > b$.

The calculations of Dubos *et al.* (1999) for an open tonehole of short height was based on a rough approximation of Green's function, whereas it was correct for a closed tonehole. The FEM results for the series equivalent lengths confirm this difference; the theoretical formula by Dubos *et al.* (1999) better matches the FEM results for a closed tonehole.

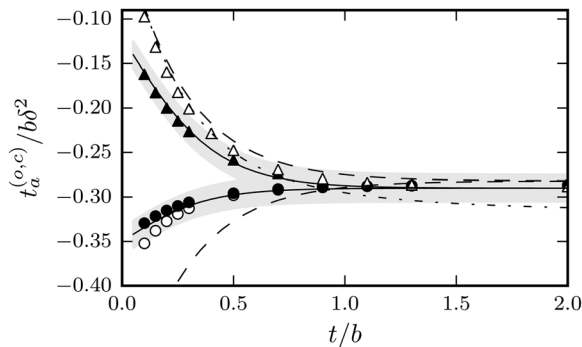


FIG. 14. Series length correction $t_a^{(o,c)}/b\delta^2$ as a function of t/b for $\delta = 1.0$ for open and closed toneholes of both types. FEM results: Unflanged tonehole (filled markers) and tonehole on a thick pipe (unfilled markers); open toneholes (circles) and closed toneholes (triangles). Data fit formulas: Equations (33) and (34) (solid line). Theory: Equations (15) and (18) (dashed line), Eq. (17) (dashed-dotted line). Validity range in gray.

VII. IMPACT OF CONICITY

Previous studies of woodwind instrument toneholes have only considered holes in cylindrical waveguides. Although the influence of an air column taper on the TM parameters of the tonehole is likely small, because the taper angle of woodwind instruments is small, the magnitude of this potential effect is unknown.

A tonehole on a conical bore is no longer symmetric. In this situation, the model represented by Eq. (2) is modified as follows:

$$\mathbf{T}_{\text{hole}} = \begin{bmatrix} 1 & \bar{Z}_{a_u} \\ 0 & 1 \end{bmatrix} \begin{bmatrix} 1 & 0 \\ 1/\bar{Z}_s & 1 \end{bmatrix} \begin{bmatrix} 1 & \bar{Z}_{a_d} \\ 0 & 1 \end{bmatrix} = \begin{bmatrix} 1 + \bar{Z}_{a_u}/\bar{Z}_s & \bar{Z}_{a_u} + \bar{Z}_{a_d} + \bar{Z}_{a_u}\bar{Z}_{a_d}/\bar{Z}_s \\ 1/\bar{Z}_s & 1 + \bar{Z}_{a_d}/\bar{Z}_s \end{bmatrix}, \quad (35)$$

where \bar{Z}_{a_u} and \bar{Z}_{a_d} are the series impedances for the upstream and downstream halves of the tonehole, respectively.

In a manner similar to that for toneholes on cylindrical bores, the TM of the tonehole on a conical bore is obtained using the FEM. The conical system only has one symmetry plane, thus requiring one-half of the model to be simulated (compared with one-quarter in the cylindrical case). This revised procedure was first validated using a cylindrical model and the exact same results (within 0.1%) as reported in the previous section were obtained. Notably, the upstream and downstream values of the series equivalent lengths were identical.

The transfer matrix \mathbf{T}_{hole} of the tonehole was obtained from the transfer matrix \mathbf{T} of the simulated system by multiplying this matrix by the inverse of the TM of the two segments of truncated cones, $\mathbf{T}_{\text{cone}_u}$ and $\mathbf{T}_{\text{cone}_d}$,

$$\mathbf{T}_{\text{hole}} = \mathbf{T}_{\text{cone}_u}^{-1} \mathbf{T} \mathbf{T}_{\text{cone}_d}^{-1}, \quad (36)$$

where the TM of a conical waveguide can be found in Fletcher and Rossing (1998)

The objectives are to determine whether or not the shunt impedance \bar{Z}_s is different from that derived for a cylindrical bore and to determine the effect of the asymmetry on the values of \bar{Z}_{a_u} and \bar{Z}_{a_d} . The tonehole parameters were obtained for two conical waveguides with taper angles of 3° and 6° . Bassoons and oboes have respective taper angles of approximately 0.8° and 1.5° . Alto and soprano saxophones have respective taper angles of approximately 3° and 4° . A few saxophone toneholes are located in the beginning of the flaring bell where the angle increases. An angle of 6° is a reasonable practical limit.

As for toneholes on a cylindrical bore, a data-fit formula for the shunt equivalent length of the open tonehole is obtained from the simulation data (with the same set of parameters). The maximal observed difference between the two data-fit formulas was $4 \times 10^{-5} b$. This is a very small difference and the authors thus conclude that the shunt length corrections are not significantly changed relative to their values on a cylindrical bore.

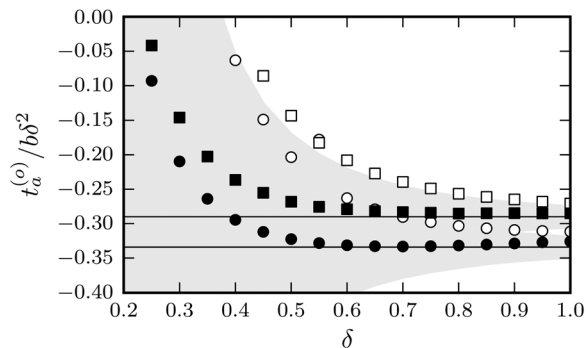


FIG. 15. Series length correction $t_a^{(o)}/b\delta^2$ as a function of δ for a tonehole on a conical bore: With a taper angle of 3° (filled markers) and a taper angle of 6° (unfilled markers). FEM results: Sum of upstream and downstream parts for tall $t=2b$ (squares) and short $t=0.1b$ (circles) toneholes. Data fit formula Eq. (33) (solid line).

The sum of the upstream and downstream series length corrections, $t_a^{(o)}/b\delta^2$, computed for a conical bore with a taper angle of 3° and 6° , is shown in Fig. 15. For the smaller taper angle and $\delta > 0.5$, the FEM results are close to the values given by Eq. (33). The results for smaller toneholes differ more significantly from Eq. (33) although they remain well within the validity range and are thus considered negligible. The results for a cone with a taper angle of 6° reveal discrepancies from Eq. (33) that are more significant, even for higher values of δ , with simulated values falling on or slightly outside the range of validity. However, this taper angle is beyond most practical cases in musical instruments.

The conclusion of this analysis is that the use of TM parameters developed for toneholes on cylindrical bores is valid for conical bores, at least up to an angle of 3° and probably for most applications in musical instruments.

VIII. CONCLUSION

A method to derive the transfer matrix parameters of a discontinuity in a waveguide was developed and applied successfully to the case of woodwind instrument toneholes. Simple polynomial fit formulas were developed that match the FEM results. These results confirm the validity of the equations from the literature for tall toneholes ($t > b$). For large-diameter toneholes of shorter height, the shunt equivalent length of an open tonehole increases more with frequency than predicted by previous expressions. This can be explained by a frequency-dependent inner length correction. The series equivalent length increases in magnitude as the tonehole height decreases, but not as much as predicted by previous formulas.

For closed toneholes, the formulations found in the literature are correct but new equations are proposed that better match the FEM results. The reduction in the magnitude of the series equivalent length for short toneholes must be accounted for when calculating the resonance frequencies of woodwind instruments, particularly for the lowest notes, because of the cumulative effect of this term; otherwise, the calculated resonances will be higher than they should be.

The possible impact of a main bore taper (angles of 3° and 6°) on the characterization of toneholes was estimated from FEM simulations. The shunt equivalent length was found to be unaffected by a bore taper. The series equivalent length term differs to some extent, although it remains within the estimated maximal tolerable error for a taper angle of 3° . Thus, the parameters of a tonehole on a cylindrical bore can be used safely on a conical bore instrument, at least up to a taper angle of 3° .

This method can be applied to the case of a hanging key above a tonehole, a tonehole with undercutting, a tonehole with rolled chimney or to other particular geometric features. Future work will include an experimental verification of the transfer matrix parameters of open and closed toneholes of short height.

ACKNOWLEDGMENTS

Many thanks to Jean-Pierre Dalmont and his colleagues for sharing their experimental data and to the anonymous reviewers for valuable feedback and suggestions. A “Fonds québécois de la recherche sur la nature et les technologies” (FQRNT) doctoral scholarship funded the first author (A.L.) during much of this work, as well as Natural Sciences and Engineering Research Council of Canada (NSERC) Discovery and Discovery Accelerator Supplement grants for subsequent funding. We also acknowledge support from the Centre for Interdisciplinary Research in Music Media and Technology (CIRMMT).

- Bayliss, A., Gunzburger, M., and Turkel, E. (1982). “Boundary conditions for the numerical solution of elliptic equations in exterior regions,” *SIAM J. Appl. Math.* **42**, 430–451.
- Caussé, R., Kergomard, J., and Lurton, X. (1984). “Input impedance of brass musical instruments—comparison between experimental and numerical models,” *J. Acoust. Soc. Am.* **75**, 241–254.
- Dalmont, J., and Nederveen, C. J. (2001). “Radiation impedance of tubes with different flanges: Numerical and experimental investigations,” *J. Sound Vib.* **244**, 505–534.
- Dalmont, J., Nederveen, C., Dubos, V., Ollivier, S., Meserette, V., and te Slighte, E. (2002). “Experimental determination of the equivalent circuit of an open side hole: Linear and non linear behaviour,” *Acta Acust. Acust.* **88**, 567–575.
- Debut, V., Kergomard, J., and Laloö, F. (2005). “Analysis and optimisation of the tuning of the twelfths for a clarinet resonator,” *Appl. Acoust.* **66**, 365–409.
- Dickens, P. A. (2007). “Flute acoustics: Measurement, modelling and design,” Ph.D. thesis, University of New South Wales.
- Dubos, V., Kergomard, J., Khettabi, A., Dalmont, J., Keefe, D., and Nederveen, C. (1999). “Theory of sound propagation in a duct with a branched tube using modal decomposition,” *Acust. Acta Acust.* **85**, 153–169.
- Fletcher, N., and Rossing, T. (1998). *The Physics of Musical Instruments*, 2nd ed. (Springer, New York).
- Fletcher, N. H. (1999). “The nonlinear physics of musical instruments,” *Rep. Progr. Phys.* **62**, 723–764.
- Givoli, D., and Neta, B. (2003). “High-order non-reflecting boundary scheme for time-dependent waves,” *J. Comput. Phys.* **186**, 24–46.
- Hartmann, W. M. (1996). “Pitch, periodicity, and auditory organization,” *J. Acoust. Soc. Am.* **100**, 3491–3502.
- Kampinga, W., Wijnant, Y., and de Boer, A. (2010). “Performance of several viscothermal acoustic finite elements,” *Acta Acust. Acust.* **96**, 115–124.
- Keefe, D. (1982a). “Experiments on the single woodwind tonehole,” *J. Acoust. Soc. Am.* **72**, 688–699.
- Keefe, D. (1982b). “Theory of the single woodwind tonehole,” *J. Acoust. Soc. Am.* **72**, 676–687.

- Keefe, D. (1990). "Woodwind air column models," *J. Acoust. Soc. Am.* **88**, 35–51.
- Lefebvre, A. (2010). "Computational acoustic methods for the design of woodwind instruments," Ph.D. thesis, McGill University, Quebec, Canada.
- Levine, H., and Schwinger, J. (1948). "On the radiation of sound from an unflanged circular pipe," *Phys. Rev.* **73**, 383–406.
- Nederveen, C. (1998). *Acoustical Aspects of Woodwind Instruments*, revised ed. (Northern Illinois University Press, DeKalb, IL).
- Nederveen, C., Jansen, J., and van Hassel, R. R. (1998). "Corrections for woodwind tonehole calculations," *Acust. Acta Acust.* **84**, 957–966.
- Norris, A. N., and Sheng, I. C. (1989). "Acoustic radiation from a circular pipe with an infinite flange," *J. Sound Vib.* **135**, 85–93.
- Pierce, A. D. (1989). *Acoustics, An Introduction to Its Physical Principles and Applications* (Acoustical Society of America, Woodbury, NY), Chap. 7, pp. 316–319.
- Tsynkov, S. V. (1998). "Numerical solution of problems on unbounded domains. a review," *Appl. Numer. Math.* **27**, 465–532.